Assessment of MDA and 8-OHdG expressions in ovine pulmonary adenocarcinomas by immunohistochemical and immunofluorescence methods

Emin Karakurt[1,a], Enver Beytut[1,b], Serpil Dağ[1,c], Hilmi Nuhoğlu[1,d], Ayfer Yıldız[1,e], Emre Kurtbaş[2,f]

Kafkas University, [1]Faculty of Veterinary Medicine, Department of Pathology, [2]Institute Health Sciences, Kafkas University, Kars, Turkey

ORCIDs: [a]0000-0003-2019-3690; [b]0000-0003-3360-2940; [c]0000-0001-7667-689X; [d]0000-0003-2530-2542; [e]0000-0002-6569-5435; [f]0000-0002-9752-194X

Received July 12, 2021
Accepted June 14, 2022

Abstract

This study aimed to reveal the presence of reactive oxygen species (ROS)-induced lipid peroxidation and DNA damage in ovine pulmonary adenocarcinomas (OPA) by evaluating malondialdehyde (MDA) and 8-hydroxy-2-deoxyguanosine (8-OHdG) expressions by immunohistochemical and immunofluorescence methods. Lung tissue samples were collected from 26 sheep brought to the Pathology Department for routine diagnosis. Lung tissues were fixed in 10% neutral buffered formalin, following routine procedures tissues were stained with hematoxylin and eosin. Avidin-Biotin Peroxidase method was used as immunohistochemical staining. Indirect immunofluorescence method was applied to the sections. Tumoral cells showed acinar, papillary or mixed type patterns. Only 2 of 20 cases metastasized to regional lymph nodes. All OPAs were immune positive for Jaagsiekte Sheep Retrovirus Capsid Protein (JSRV CA), MDA and 8-OHdG. The control group was negative for JSRV CA, MDA and 8-OHdG expressions. Malondialdehyde and 8-OHdG immune positive cells were statistically increased in the OPA group compared to the control group. In conclusion, our results demonstrate that higher MDA and 8-OHdG expressions in sheep with OPA suggest that OPA may be closely related to lipid peroxidation and oxidative DNA damage.

DNA damage, lipid peroxidation, sheep, jaagsiekte, oxidative stress

Ovine pulmonary adenocarcinoma (OPA), also known as ovine pulmonary carcinoma, sheep pulmonary adenomatosis and jaagsiekte, is an infectious lung cancer of sheep caused by Jaagsiekte sheep retrovirus (JSRV) (Scott et al. 2018; De Las Heras et al. 2021). The virus is responsible for the oncogenic transformation and infection of bronchiolar and alveolar epithelial cells, namely type 2 pneumocytes and Clara cells (Sun et al. 2017; Belalmi et al. 2020; Hu et al. 2020). Ovine pulmonary adenocarcinoma is spread mostly through the respiratory route via the inhalation of the virus. DNA of JSRV has also been identified in milk and colostrum of ewes, suggesting that lambs may be exposed to the virus when suckling (Youssef et al. 2015; Miller et al. 2017). The incubation period of natural cases is quite long and ranges from 2 to 4 years, so the disease is more common in adult sheep (Toma et al. 2020). Ovine pulmonary adenocarcinoma is diagnosed not only in sheep but also in goats (Zhang et al. 2014). Progressive emaciation, weight loss, dyspnoea, polypnoea, coughing, profuse fluid accumulation in the lungs that drains from the nostrils when the sheep's head is lowered are the most important clinical features of OPA (Sonawane et al. 2016; Karagianni et al. 2019; Mansour et al. 2019). In terms of pathological and epidemiological features, OPA is similar to various pulmonary adenocarcinomas in humans, such as bronchoalveolar carcinoma (BAC), therefore, it is a very useful animal tumour model for pulmonary carcinogenesis (Hudachek et al. 2010; Humann-Ziehank et al. 2011; Sozmen and Beytut 2012). Postmortem findings,

Address for correspondence:
Emin Karakurt
Department of Pathology
Faculty of Veterinary Medicine
Kafkas University
36100 Kars, Turkey

Phone: +90 474 242 68 36/5152
E-mail: mehmeteminkarakurt@hotmail.com
http://actavet.vfu.cz/

histopathological and immunohistochemical examinations are highly reliable in the diagnosis of OPA (Liu et al. 2016; De Las Heras et al. 2021).

Oxidative stress refers to an imbalance in which reactive oxygen species (ROS) production exceeds the capacity of antioxidant defense systems and causes dysregulation of redox signalling and/or damage to important macromolecules such as DNA, proteins, and lipids (Srivastava et al. 2010; Gào et al. 2019; Zalewska-Ziob et al. 2019). Oxidative stress is involved in the pathogenesis of various diseases, especially cancer (Kaynar et al. 2005). In this context, oxidative stress is known to play a regulatory role in tumour growth and progression, including genomic instability, oncogene activation, and angiogenesis (Otsmane et al. 2018). Lipid peroxidation (LPO) is the reaction between ROS and polyunsaturated fatty acids (PUFAs) from oxidation, resulting in various changes in the structure and permeability of the lung membrane, which in turn contributes to the carcinogenesis process (Gęgotek et al. 2016; Sunnetcioglu et al. 2016). Malondialdehyde (MDA) is one of the end products of LPO and is an important marker of oxidative damage (Esme et al. 2008; Peddireddy et al. 2012). Reactive oxygen species cause DNA damage and induce genetic changes at all stages of carcinogenesis, such as initiation, promotion, and progression (Inoue et al. 1998; Ilonen et al. 2009). 8-hydroxy-2-deoxyguanosine (8-OHdG) is the most sensitive marker of ROS-induced oxidative DNA damage and causes GC ➔ TA transversion mutations (An et al. 2019; Gào et al. 2019). The increase in 8-OHdG levels is closely related to many pathological conditions including breast cancer, lung cancer, bladder cancer, colorectal cancer and prostate cancer (Peddireddy et al. 2012; An et al. 2019).

In this study, it was aimed to reveal the presence of ROS-induced lipid peroxidation and DNA damage in OPA, which is an important lung cancer in sheep, by evaluating MDA and 8-OHdG expressions by immunohistochemical methods.

Materials and Methods

Animals

The material of this study consisted of lung and lymphoid tissue samples of 20 OPA and 6 control samples brought to our department for routine histopathological diagnosis. The ethical approval for this study was obtained from the Kafkas University Animal Experimentals Local Ethics Committee (authorization number KAU-HADYEK-2021/060).

Histopathological examinations

Lung and lymphoid tissue samples were fixed in 10% buffered formaldehyde solution (Sigma-Aldrich, St. Louis, Missouri, USA), processed routinely, embedded in paraffin wax (Sigma-Aldrich), sectioned at 5 µm, stained with haematoxylin-eosin (HE), examined under a light microscope (Olympus Bx53, Hamburg, Germany) and photographed to detect histopathological changes.

Immunohistochemical and immunofluorescence examinations

The avidin-biotin-peroxidase method was used for immunohistochemistry. Slides were deparaffinized and rehydrated in graded alcohols. The sections were treated with 3% hydrogen peroxide solution in phosphate-buffered saline (PBS) for 15 min to prevent endogenous peroxidase activity, then boiled in citrate buffer solution (pH 6) for 25 min in an 800-Watt microwave oven for antigen retrieval. The sections were incubated for 10 min with non-immune serum (Thermo Scientific Histostain-Plus IHC Kit, HRP, broad-spectrum, REF: TP-125-HL, Waltham, Massachusetts, USA) at room temperature to prevent nonspecific staining. Diluted antibodies (Jaagsiekte Sheep Retrovirus Capsid Protein [JSRV CA], supplied by Prof. Massimo Palmarini, dilution of 1/1500; 8-OHdG, Bioss Antibodies, bs-1278R, dilution of 1/800, Woburn, Massachusetts, USA; MDA, Abcam, ab6463, dilution of 1/1500, Cambridge, United Kingdom) were incubated overnight in a refrigerator at 4 °C after which the sections were washed 3 × in PBS for 3 min. The biotinylated secondary antibody (Thermo Scientific, Histostain-Plus IHC Kit, HRP, broad-spectrum, REF: TP-125-HL) was applied at room temperature for 10 min. After washing in PBS for 3 min, all sections were incubated with peroxidase-bound streptavidin (Thermo Scientific, Histostain-Plus IHC Kit, HRP, broad-spectrum, REF: TP-125-HL) for 10 min at room temperature. A solution of 3,3'-diaminobenzidine (DAB) tetrahydrochloride (Thermo Scientific, REF: TA-125-HD) was used as a chromogen for 15 min. For negative control, lung tissues with OPA was used. Primary antibodies were omitted from the negative control sections treated with diluted normal serum. The prepared slides were examined under a light microscope and photographed. In the immunofluorescent method, after the primary antibody incubation, fluorescein isothiocyanate (FITC)-labelled secondary antibody (goat anti-rabbit IgG [H+L] secondary antibody, FITC cat:31635, Invitrogen, Waltham, Massachusetts, USA) was incubated for 40 min in the dark at a 1/50

dilution. After incubation, it was washed with distilled water for 3 × 5 min and covered with mounting medium 4',6-diamidino-2-phenylindole (DAPI) (Abcam ab104139, Cambridge, United Kingdom) and photographed by taking the coordinates with a fluorescent microscope. The coverslips of the photographed sections were opened with distilled water and the tissues were HE stained. In HE staining, photographs were taken from the areas in the same coordinates as in the immunofluorescence staining and combined with the immunofluorescent positive areas with Adobe Photoshop CC 2019 program (San Jose, California, USA).

MDA and 8-OHdG immunopositive expressions were analysed by examining 3 representative fields of labelled neoplastic cells at a × 40 magnification. Rating systems were designated as negative (–) 0%, low (+) 1–10%, moderate (++) 11–59% or severe (+++)> 60%.

Statistical analysis

Mann-Whitney U test was used to compare OPA and control groups according to positive cell scoring. Obtained results were presented as mean ± standard error of the mean (SEM). Statistical analyzes were performed using the SPSS® (Version 26.0, Chicago, IL, USA) program. The differences between the groups after statistical analysis were considered significant if they were at a $P < 0.05$ level.

Results

Histopathological results

In the histopathological examination of the tumours, it was observed that the alveolar lumens were typically dilated in the lung tissue and the alveolar lumens (lepidic growth) were filled with foci of papillary or acinar neoplastic proliferation of columnar or cuboidal tumoral cells replacing type 2 pneumocytes. The same type of growth patterns were also present in the bronchiolar walls. Alveolar lumens in or adjacent to tumoral areas were found to be filled with macrophages. The thin tumour stroma was thickened due to lymphocyte, plasma and connective tissue components. In some areas, myxoid growths with epithelial components were visible. Tumour cells were well differentiated and mitotic figures were negligible. Metastases to regional lymph nodes were detected in only 2 cases, and neoplastic cells were found to grow in papillary or acinar patterns in these lymphoid tissues, similar to primary tumour foci (Plate III-IV, Figs 1–3).

Immunohistochemical and immunofluorescence results

All OPA cases were positive for JSRV CA immunoreactivity and yellow-brownish reactions were especially in the cytoplasm of tumoral cells (Fig. 4., Plate IV) MDA and 8-OHdG expressions were statistically increased in the OPA group compared to the control group (Table 1). MDA positive reactions were observed in tumoral cells forming papillary and acinar structures. The reactions were intracytoplasmic (Plate V, Fig. 5a). In some areas, alveolar macrophages were also found to give a positive reaction. In metastatic cases, intense intracytoplasmic MDA expressions were detected in the cytoplasm of tumour cells, similar to primary tumour foci (Fig. 5b). Strong 8-OHdG immunoreactivity was observed in glandular and papillary neoplastic proliferation foci, and in the cytoplasm of tumoral cells. Similar to MDA, alveolar macrophages in the tumoral areas were immunopositive for the 8-OHdG reaction. In the metastic area around the lymphoid tissue, the neoplastic cells were stained positively with 8-OHdG, consistent with the primary tumour foci (Plate V, Fig. 6a-b).

Table 1. Mean ± standard error values of OPA and control groups.

Groups	MDA	8-OHdG
OPA	2.80 ± 0.09^{a}	2.35 ± 0.13^{a}
Control	0 ± 0^{b}	0 ± 0^{b}

[a,b] - Different superscripts in each column indicate significant differences between the groups ($P < 0.05$); MDA – malondialdehyde; 8-OHdG - 8-hydroxy-2-deoxyguanosine; OPA - ovine pulmonary adenocarcinoma

MDA expressions were detected diffusely located in the cytoplasm of tumoral cells. In the lymph node, similar to the lung tissue findings, intracytoplasmic diffuse positive reactions were observed in the cytoplasm of the cells in the neoplastic proliferation foci. 8-OHdG positive reactions were observed in glandular and papillary neoplastic proliferation foci within alveolar lumens. Similar to MDA findings, in the metastic area around the lymphoid tissue, the neoplastic cells were diffusely stained with 8-OHdG (Plate V-VI, Figs 7–8).

In immunohistochemical and immunofluorescence (IFC) assays, the control group was negative in terms of MDA and 8-OHdG immunoreactivity. The control group did not give a positive reaction in terms of JSRV CA expression either (Plate VI, Fig. 9).

Discussion

According to the data of The World Organization for Animal Health (OIE), OPA is considered to be the most important disease that can affect international trade (Zhang et al. 2014). Diagnosis of OPA is possible when clinical signs or tumours are detected, and the presence of JSRV can be supported by immunoblotting, ELISA, or polymerase chain reaction (PCR) in lung fluid or tumours, however, routine testing for preclinical diagnosis of JSRV infection is not available (Sonawane et al. 2016). In the absence of serological testing and cell culture for JSRV isolation, there is no confirmatory laboratory method for premortem diagnosis of OPA in affected animals, and a complete diagnosis can only be made on the basis of herd history, clinical signs, and postmortem lesions (Sonawane et al. 2016; De Las Heras et al. 2021). Disease can be confirmed by PCR examination. However, the ability of this method to identify only a few infected animals is limited (Liu et al. 2016). A complete diagnosis is only possible with postmortem histopathological examination. Immunohistochemical methods may also be useful in the diagnosis of the disease (Toma et al. 2020; De Las Heras et al. 2021). The characteristic histopathological (Humann-Ziehank et al. 2011; Youssef et al. 2015; Mansour et al. 2019) and immunohistochemical findings (Hudachek et al. 2010; Sun et al. 2017; Belalmi et al. 2020) of OPA were observed in sheep in this study, which were consistent as previously reported.

The most common causes of cancer death are lung, liver, and stomach cancers (Otsmane et al. 2018; An et al. 2019; Ferlay et al. 2021). Lung cancers are divided into two subtypes, non-small-cell lung cancer (NSCLC) and small-cell lung cancer (SCLC). More than 85% of lung cancers are NSCLC and the remaining 15% are SCLC (Zalewska-Ziob et al. 2019). The most common histological subtypes of NSCLCs are squamous cell lung carcinoma (SCC) and adenocarcinoma (AC) (Gęgotek et al. 2016). Lung tissue is a primary organ that is constantly in contact with higher oxygen pressure, environmental irritants and pollutant including oxidants than other tissues and exhibits a special sensitivity to ROS due to its large surface area (Peddireddy et al. 2012; Gęgotek et al. 2016; Zalewska-Ziob et al. 2019). Oxidative stress occurs in a cell or tissue when the concentration of ROS produced exceeds that cells antioxidant capacity (Oral et al. 2015; Sunnetcioglu et al. 2016). It is known that oxidative stress is involved in all stages of carcinogenesis such as initiation, promotion, and progression and is an important factor for lung cancers (Kaynar et al. 2005). Reactive oxygen species cause serious tissue damage by reacting with all biological macromolecules such as lipids, proteins, and nucleic acids (Srivastava et al. 2010). Data from recent studies show that the presence of ROS plays an important role in tumour development (Sunnetcioglu et al. 2016). Malondialdehyde is an end-product of LPO of membrane PUFAs by free radicals and behaves like as tumour promoter and co-carcinogenic agent because of its high cytotoxicity and inhibitory action against protective enzymes (Kaynar et al. 2005; Esme et al. 2008; Otsmane et al. 2018). In the literature review, no study was found in which the lipid peroxidation status of OPAs was evaluated by means of MDA expression. In human medicine, MDA levels were evaluated in different cancer stages and different lung cancers such as NSCLC, SCLC, AC and large cell carcinoma, and it was reported that MDA levels increased significantly compared to the control groups (Gęgotek et al. 2016; Sunnetcioglu et al. 2016; Otsmane et al. 2018). In addition, it has been reported that MDA levels increase in parallel with the progression of cancer stages (Esme et al. 2008; Srivastava et al. 2010; Peddireddy et al. 2012). Unlike these studies, Zalewska-Ziob et al. (2019) found that there was no significant difference

in MDA concentration between tumour tissue and adjacent normal tissue in patients with NSCLC. In accordance with the literature data (Gęgotek et al. 2016, Sunnetcioglu et al. 2016; Otsmane et al. 2018), MDA expression in the present study was significantly increased in the OPAs which showed significant pathological and epidemiological similarities with BAC compared to the control group. The presence of MDA expression in both primary and secondary tumoral areas was found in 2 cases that metastasized to regional lymph nodes (Esme et al. 2008; Srivastava et al. 2010; Peddireddy et al. 2012). In addition to tumoral cells, alveolar macrophages were also positive for MDA expression. In response to different stimuli, alveolar macrophages release ROS and inflammatory mediators, thereby promoting inflammation (Aaam and Fonnum 2007). Phagocytes such as neutrophils and macrophages produce ROS during phagocytosis (Forman and Torres 2002). We believe that this immunoreactivity in alveolar macrophages in the tumour microenvironment is particularly related to the elimination of invading microorganisms by oxidative burst mediated by nicotinamide adenine dinucleotide phosphate oxidase (Canton et al. 2021). In addition, ROS released by alveolar macrophages may have a significant role in the inflammatory response around tumoral foci (Aaam and Fonnum 2007). 8-OHdG is one of the most important forms of DNA damage induced by ROS and is a highly reliable and useful biomarker for the assessment of oxidative DNA damage (Inoue et al. 1998; Cao et al. 2016). The clinical significance of 8-OHdG is still controversial, with some researchers linking increased 8-OHdG expression to poor prognosis, while others report negative 8-OHdG expression to be associated with aggressive cancer phenotype (An et al. 2019). Ilonen et al. (2009) found no significant difference in 8-OHdG content between NSCLC, non-malignant tissues and control samples. In a similar study, Sunnetcioglu et al. (2016) observed an increase in 8-OHdG levels in the lung cancer group compared to the control group, but reported that this increase was non-significant. An et al. (2019) reported that 8-OHdG expression in NSCLCs indicates good prognosis. Contrary to these studies, there are also studies reporting that 8-OHdG levels are significantly increased in lung cancers such as SCC and AC compared to the control group (Inoue et al. 1998; Gęgotek et al. 2016). In lung cancers such as NSCLC, SCLC and AC, 8-OHdG levels have been found to be closely related to cancer grades and stages and to increase in parallel with these (Peddireddy et al. 2012; Cao et al. 2016). In veterinary medicine, no literature data could be found in which 8-OHdG expressions in OPAs were evaluated by immunohistochemical and immunofluorescent methods. Similar to the literature data (Inoue et al. 1998; Peddireddy et al. 2012; Cao et al. 2016; Gęgotek et al. 2016), in the present study, it was determined that 8-OHdG expressions were significantly increased in the OPA group compared to the control group. Similar to MDA results, tumour cells were found to be positive for 8-OHdG expression in the metastatic focus in the lymph node in 2 cases that metastasized.

In conclusion, our results demonstrate that higher MDA and 8-OHdG expressions in sheep with OPA suggest that OPA may be closely related to lipid peroxidation and oxidative DNA damage. Oxidative stress indicators such as MDA and 8-OHdG are thought to be very useful in the diagnosis of OPA. In addition, it is possible that antioxidant therapy may also be effective in regressing the disease.

References

Aam BB, Fonnum F 2007: Carbon black particles increase reactive oxygen species formation in rat alveolar macrophages *in vitro*. Arch Toxicol **81**: 441-446

An AR, Kim KM, Park HS, Jang KY, Moon WS, Kang MJ, Lee YC, Kim JH, Chae HJ, Chung MJ 2019: Association between expression of 8-OHdG and cigarette smoking in non-small cell lung cancer. J Pathol Transl Med **53**: 217-224

Belalmi NEH, Sid N, Bennoune O, Ouhida S, Heras ML, Leroux C 2020: Evidence of jaagsiekte sheep retrovirus-induced pulmonary adenocarcinoma in Ouled Djellal breed sheep in Algeria. Vet Res Forum **11**: 93-95

Canton M, Sánchez-Rodríguez R, Spera I, Venegas FC, Favia M, Viola A, Castegna A 2021: Reactive oxygen species in macrophages: sources and targets. Front Immunol **12**: 734229
Cao C, Lai T, Li M, Zhou H, Lv D, Deng Z, Ying S, Chen Z, Li W, Shen H 2016: Smoking-promoted oxidative DNA damage response is highly correlated to lung carcinogenesis. Oncotarget **7**: 18919-18926
De Las Heras M, Borobia M, Ortín A 2021: Neoplasia-associated wasting diseases with economic relevance in the sheep industry. Animals (Basel) **11**: 381
Esme H, Cemek M, Sezer M, Saglam H, Demir A, Melek H, Unlu M 2008: High levels of oxidative stress in patients with advanced lung cancer. Respirology **13**: 112-116
Ferlay J, Colombet M, Soerjomataram I, Parkin DM, Piñeros M, Znaor A, Bray F 2021: Cancer statistics for the year 2020: An overview. Int J Cancer **149**: 778-789
Forman HJ, Torres M 2002: Reactive oxygen species and cell signaling: respiratory burst in macrophage signaling. Am J Respir Crit Care Med **166**: S4-S8
Gào X, Holleczek B, Cuk K, Zhang Y, Anusruti A, Xuan Y, Xu Y, Brenner H, Schöttker B 2019: Investigation on potential associations of oxidatively generated DNA/RNA damage with lung, colorectal, breast, prostate and total cancer incidence. Sci Rep **9**: 7109
Gęgotek A, Nikliński J, Žarković N, Žarković K, Waeg G, Łuczaj W, Charkiewicz R, Skrzydlewska E 2016: Lipid mediators involved in the oxidative stress and antioxidant defence of human lung cancer cells. Redox Biol **9**: 210-219
Hu Y, Ren S, He Y, Wang L, Chen C, Tang J, Liu W, Yu F 2020: Possible oncogenic viruses associated with lung cancer. Onco Targets Ther **13**: 10651-10666
Hudachek SF, Kraft SL, Thamm DH, Bielefeldt-Ohmann H, DeMartini JC, Miller AD, Dernell WS 2010: Lung tumor development and spontaneous regression in lambs coinfected with Jaagsiekte sheep retrovirus and ovine lentivirus. Vet Pathol **47**: 148-162
Humann-Ziehank E, Wolf P, Renko K, Schomburg L, Ludwig Bruegmann M, Andreae A, Brauer C, Ganter M 2011: Ovine pulmonary adenocarcinoma as an animal model of progressive lung cancer and the impact of nutritional selenium supply. J Trace Elem Med Biol **25**: S30-S34
Ilonen IK, Räsänen JV, Sihvo EI, Knuuttila A, Salmenkivi KM, Ahotupa MO, Kinnula VL, Salo JA 2009: Oxidative stress in non-small cell lung cancer: role of nicotinamide adenine dinucleotide phosphate oxidase and glutathione. Acta Oncol **48**: 1054-1061
Inoue M, Osaki T, Noguchi M, Hirohashi S, Yasumoto K, Kasai H 1998: Lung cancer patients have increased 8-hydroxydeoxyguanosine levels in peripheral lung tissue DNA. Jpn J Cancer Res **89**: 691-695
Karagianni AE, Vasoya D, Finlayson J, Martineau HM, Wood AR, Cousens C, Dagleish MP, Watson M, Griffiths DJ 2019: Transcriptional response of ovine lung to infection with jaagsiekte sheep retrovirus. J Virol **93**: e00876-19
Kaynar H, Meral M, Turhan H, Keles M, Celik G, Akcay F 2005: Glutathione peroxidase, glutathione-S-transferase, catalase, xanthine oxidase, Cu-Zn superoxide dismutase activities, total glutathione, nitric oxide, and malondialdehyde levels in erythrocytes of patients with small cell and non-small cell lung cancer. Cancer Lett **227**: 133-139
Liu Y, Zhang YF, Sun XL, Liu SY 2016: Detection of Jaagsiekte sheep retrovirus in the peripheral blood during the pre-clinical period of ovine pulmonary adenomatosis. Genet Mol Res **15**: gmr.15038521
Mansour KA, Al-Husseiny SH, Kshash QH, Jassim A 2019: Clinical-histopathological and molecular study of ovine pulmonary adenocarcinoma in Awassi sheep in Al-Qadisiyah Province, Iraq. Vet World **12**: 454-458
Miller AD, De Las Heras M, Yu J, Zhang F, Liu SL, Vaughan AE, Vaughan TL, Rosadio R, Rocca S, Palmieri G, Goedert JJ, Fujimoto J, Wistuba II 2017: Evidence against a role for jaagsiekte sheep retrovirus in human lung cancer. Retrovirology **14**: 3
Oral H, Öğün M, Kuru M, Kaya S 2015: Evaluation of certain oxidative stress parameters in heifers that were administered short therm prid. Kafkas Univ Vet Fak Derg **21**: 569-573
Otsmane A, Kacimi G, Adane S, Cherbal F, Aouichat Bouguerra S 2018: Clinico-epidemiological profile and redox imbalance of lung cancer patients in Algeria. J Med Life **11**: 210-217
Peddireddy V, Siva Prasad B, Gundimeda SD, Penagaluru PR, Mundluru HP 2012: Assessment of 8-oxo-7, 8-dihydro-2'-deoxyguanosine and malondialdehyde levels as oxidative stress markers and antioxidant status in non-small cell lung cancer. Biomarkers **17**: 261-268
Scott PR, Dagleish MP, Cousens C 2018: Development of superficial lung lesions monitored on farm by serial ultrasonographic examination in sheep with lesions confirmed as ovine pulmonary adenocarcinoma at necropsy. Ir Vet J **71**: 23
Sonawane GG, Tripathi BN, Kumar R, Kumar J 2016: Diagnosis and prevalence of ovine pulmonary adenocarcinoma in lung tissues of naturally infected farm sheep. Vet World **9**: 365-370
Sozmen M, Beytut E 2012: An investigation of growth factors and lactoferrin in naturally occurring ovine pulmonary adenomatosis. J Comp Pathol **147**: 441-451
Srivastava AN, Gupta A, Srivastava S, Natu SM, Mittal B, Negi MP, Prasad R 2010: Cisplatin combination chemotherapy induces oxidative stress in advance non small cell lung cancer patients. Asian Pac J Cancer Prev **11**: 465-471
Sun X, Du F, Liu S 2017: Modulation of autophagy in exJSRV-env-transfected cells through the Akt/mTOR and MAPK signaling pathway. Biochem Biophys Res Commun **485**: 672-678

Sunnetcioglu A, Alp HH, Sertogullarından B, Balaharoglu R, Gunbatar H 2016: Evaluation of oxidative damage and antioxidant mechanisms in copd, lung cancer, and obstructive sleep apnea syndrome. Respir Care **61**: 205-211

Toma C, Bâlteanu VA, Tripon S, Trifa A, Rema A, Amorim I, Pop RM, Popa R, Catoi C, Taulescu M 2020: Exogenous Jaagsiekte Sheep Retrovirus type 2 (exJSRV2) related to ovine pulmonary adenocarcinoma (OPA) in Romania: prevalence, anatomical forms, pathological description, immunophenotyping and virus identification. BMC Vet Res **16**: 296

Youssef G, Wallace WA, Dagleish MP, Cousens C, Griffiths DJ 2015: Ovine pulmonary adenocarcinoma: a large animal model for human lung cancer. ILAR J **56**: 99-115

Zalewska-Ziob M, Adamek B, Kasperczyk J, Romuk E, Hudziec E, Chwalińska E, Dobija-Kubica K, Rogoziński P, Bruliński K 2019: Activity of antioxidant enzymes in the tumor and adjacent noncancerous tissues of non-small-cell lung cancer. Oxid Med Cell Longev **2019**: 2901840

Zhang K, Kong H, Liu Y, Shang Y, Wu B, Liu X 2014: Diagnosis and phylogenetic analysis of ovine pulmonary adenocarcinoma in China. Virus Genes **48**: 64-73

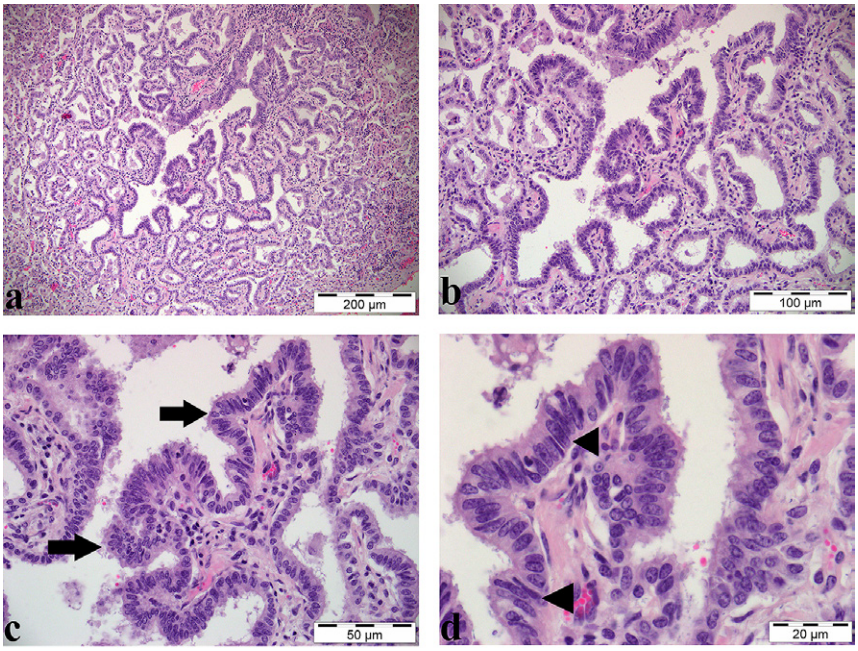

Fig. 1. Lung tissue, haematoxylin-eosin. Enlargement of alveolar lumens in different magnifications (a, b), papillary proliferations (arrows, c); and columnar tumoral cells (arrowheads, d)

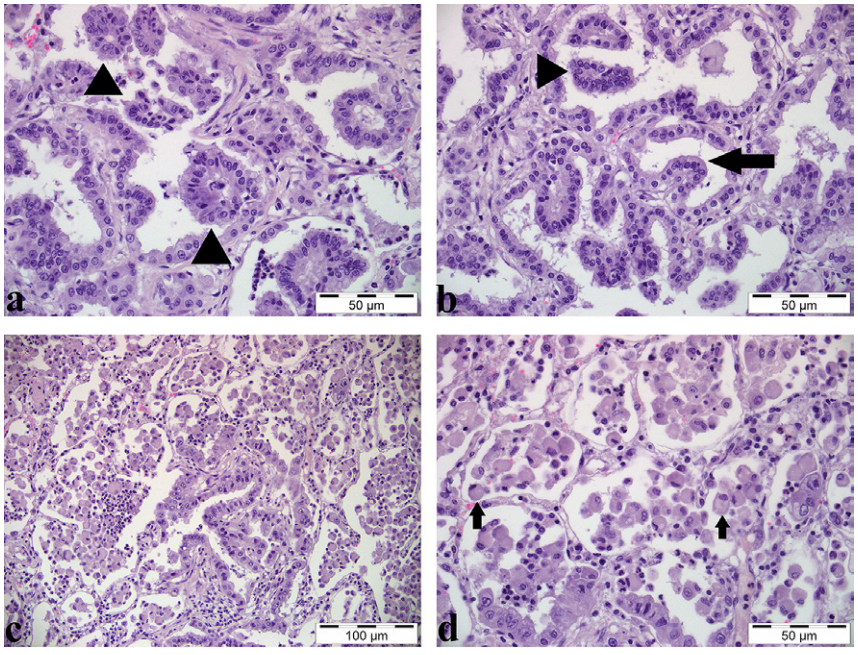

Fig. 2. Lung tissue, haematoxylin-eosin. Acinar (arrowheads, a); and papillary (arrow) neoplastic proliferation foci in alveolar lumens (b); alveolar macrophages (arrows) at different magnifications in the tumoral area (c, d)

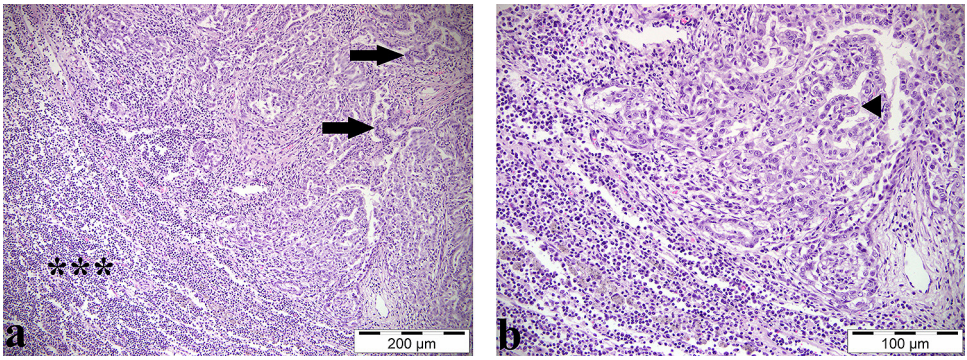

Fig. 3. Regional lymph node, haematoxylin-eosin. Lymphoid tissue (***) and neoplastic tumoral proliferations (arrows) in the metastatic area (a); papillary proliferation around the lymphoid tissue (arrowhead, b)

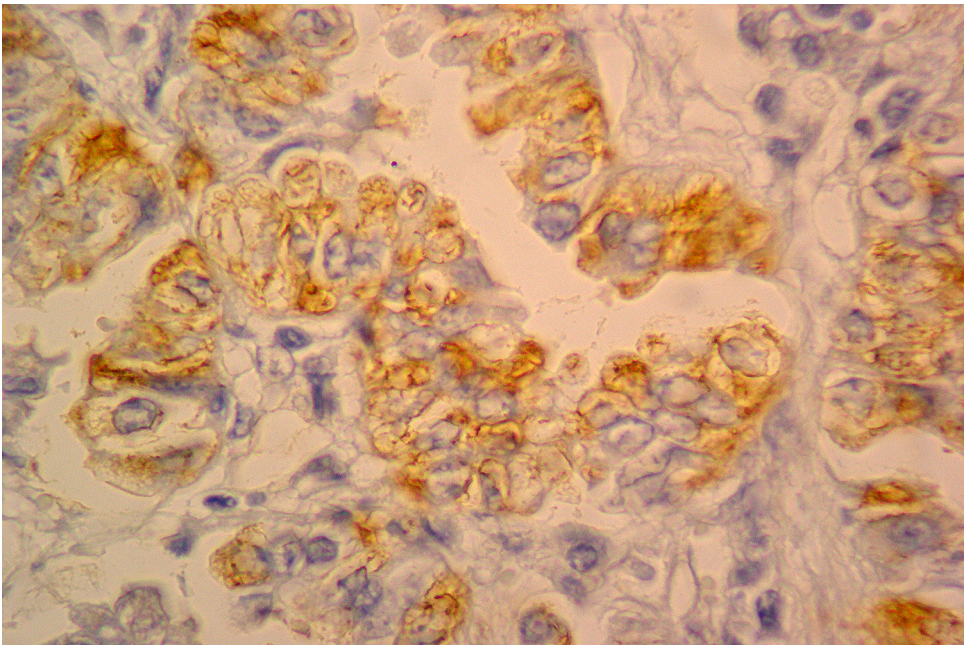

Fig. 4. Lung tissue. Intracytoplasmic positive Jaagsiekte sheep retrovirus capsid protein reactions in neoplastic cells, × 80 magnification

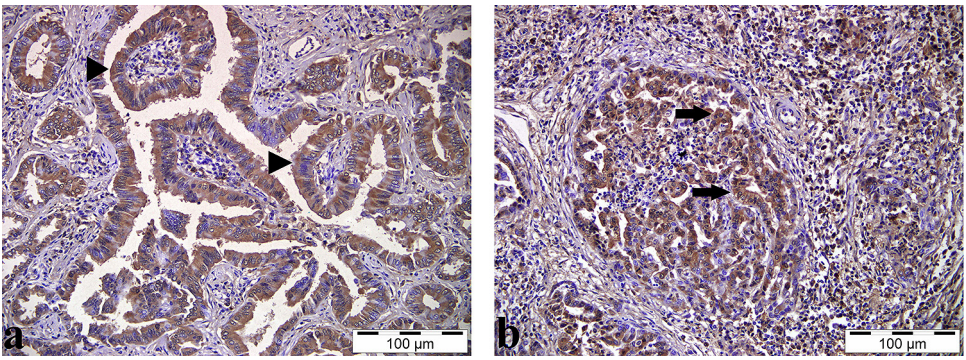

Fig. 5. Malondialdehyde, immunohistochemistry, lung tissue. Intracytoplasmic positive reactions (arrowheads) in foci of neoplastic proliferation within the dilated alveolar lumen (a); lymph node, positive immunoreactivity in the cytoplasm of tumour cells in the focus of metastasis (b)

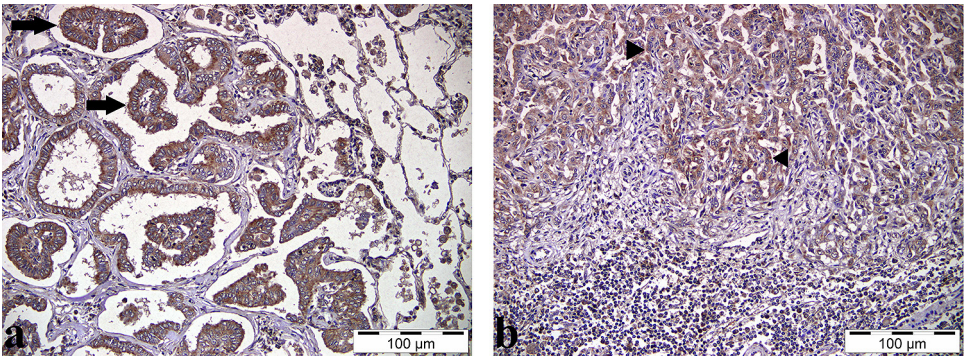

Fig. 6. 8-hydroxy-2-deoxyguanosine, immunohistochemistry, lung tissue. Positive dark Brown expressions in neoplastic glandular formations (arrows) within alveolar lumens (a); lymph node, positive brown staining in tumour focus adjacent to lymphoid tissue (b)

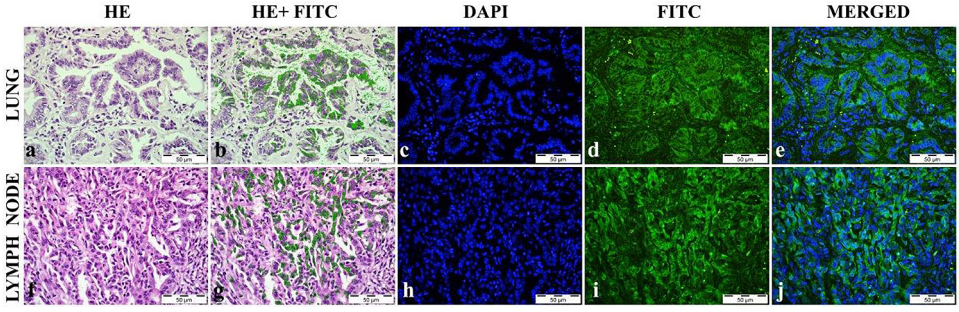

Fig 7. Malondialdehyde (MDA) positive immunofluorescence (IFC) stainings (c, d, e, h, i and j) in lung and lymph nodes; haematoxylin-eosin (HE) staining of IFC made sections (a and f), and combined HE images with IFC positive areas (b and g), Bar= 50 µm; lung IFC made area HE (a); lung HE and IFC positive area combined HE+IFC (b); lung 4',6-diamidino-2-phenylindole (DAPI) (c); MDA positive areas in lung tumor epithelial cells (d); lymph node IFC made area metastasis HE (f); lymph node metastasis HE combined with IFC positive area HE+IFC (g); lymph node metastasis DAPI (h); MDA positive areas in lymph node tumour epithelial cells (i); FITC - fluorescein isothiocyanate

Plate VI

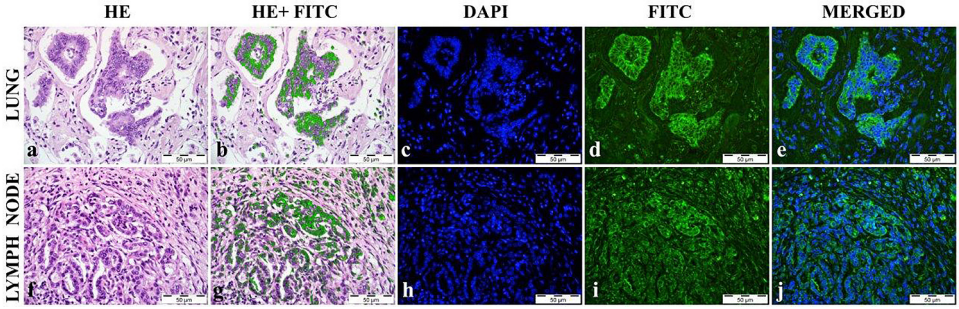

Fig. 8. 8-hydroxy-2-deoxyguanosine (8-OHdG) positive immunofluorescence (IFC) stainings (c,d,e,h,i and j) in the lungs and lymph nodes; haematoxylin-eosin (HE) staining of IFC made sections (a and f), and combined IFC areas and HE images (b and g) Bar= 50 µm; lung IFC made area HE (a); lung HE and IFC positive area combined HE+IFC (b); lung 4',6-diamidino-2-phenylindole (DAPI) (c); 8-OHdG positive areas in lung tumour epithelial cells (d); lymph node metastasis IFC made area HE (f); lymph node metastasis combined HE and IFC positive area HE+IFC (g); lymph node metastasis DAPI (h); 8-OHdG positive areas in lymph node tumor epithelial cells (i); FITC - fluorescein isothiocyanate

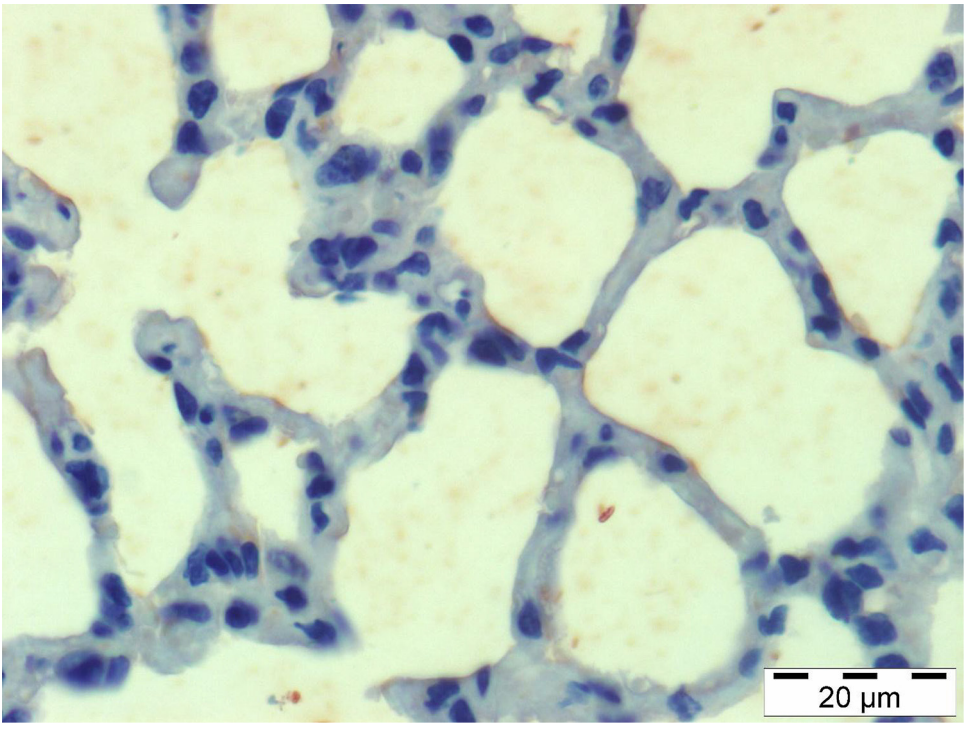

Fig. 9. Lung tissue, control group. Negative Jaagsiekte sheep retrovirus capsid protein reactions